Vortex Formation in Back-Step Flow

Adrian Mihaiescu[1], Horia Hangan[1], Anthony Straatman[1], Eduardo Wesfreid[2]

[1]**Faculty of Engineering, University of Western Ontario, London, ON, N6G 2B9, Canada**
[2]**École Supérieure de Physique et Chimie Industrielles de Paris, ESPCI-PMMH, 10, rue Vauquelin, 75231 Paris cedex 5, France**

Abstract. The structure and stability of the flow over a backward-facing step are numerically investigated. Two sets of steady-state simulations at Reynolds number between 70 and 600 are conducted: first solid walls at the lateral boundaries of the computational domain are considered and then the case of permeable lateral boundaries is studied. Potential areas for the centrifugal instability are identified using the Rayleigh criterion and computing the Görtler number. The influence of the lateral boundaries and of the inflow conditions on the vorticity field is investigated.

Key words: stability, vorticity, backward-facing step, laminar flow.

1. Introduction

The aim of this study is the investigation of the influence of the boundary conditions on the structure and stability of the laminar, steady backward-facing step flow, for low expansion ratio. The focus is the examination of the stream-wise vorticity field, which can be influenced by the presence of centrifugal instabilities in the flow.
The structure backward-facing flow step was experimentally studied by Armaly et al.[1], for a Reynolds number range covering the laminar, transition and turbulent regimes. Measurements of the instantaneous velocity were taken in vertical and horizontal plane, using a LASER-DOPPLER anemometer. The channel had the expansion ratio 2 and the aspect ratio 18. The dependency of the size of the primary and two additional recirculation zones with the Reynolds number was studied. It was found that the variation of the primary reattachment length depends on the flow regime. The horizontal profiles of the velocity proved that, despite the large aspect ratio of the channel, the flow becomes three-dimensional after a threshold value of the Reynolds number (Re=300). The mechanism of the transition to the three-dimensional state was not explained, but an interaction between the primary recirculation zone the secondary recirculation zone located on the upper wall was suggested. The experiments were backed up by two-dimensional simulations. Significant differences between the numerical and experimental results were fond for Re>300, proving that two-dimensional numerical schemes cannot accurately simulate the three-dimensional back-step flow. This result was confirmed by other numerical studies, such as Kim and Moin [2].
The structure of the three-dimensional backward-facing step flow in laminar regime was numerically studied by Williams and Baker [3]. The computational domain

was characterized by the expansion ratio 2 and aspect ratio 18, simulating the experimental conditions of Armaly et al.[1]. The study showed the formation of a walljet attached to the sidewalls at the step level. The onset to three-dimensionality of the flow was proved to be the result of the interaction of this walljet with the two-dimensional flow in the central zone of the flow domain.
The first numerical study focused on the stability of the backward-facing step flow was conducted by Kaiktsis et al.[4]. The expansion ratio was 2 and periodical boundary conditions were applied in the span-wise direction. The results showed that the transition to the three-dimensional state occurs at Re=700, corresponding to both primary and secondary bifurcations points. Thus, all the unsteady states of the flow are three-dimensional, and can develop only for Re>700. The onset to three-dimensionality originates at the boundaries between the separation zones and the mainstream flow.
The linear stability analysis of the back-step flow conducted by Barkley et al.[5] proved that the first bifurcation to a steady, three-dimensional state occurs Re_c=748. The second bifurcation point is not found, but it is suggested that it cannot occur for Re<1500. The wavelength of the unstable perturbation corresponding to the firs bifurcation was found $\lambda_c = 6.9$ (in dimensionless form, based on the step height). The instability originates from a zone located in the vicinity of the step plane. It is suggested that the instability mechanism is centrifugal. Two possible explanations for the discrepancies between their results and the conclusions of [4] are proposed. First, the instability observed by Kaiktsis et al.[4] are convective caused by the poor resolution of the numerical procedure. Then the possible presence of subcritical instabilities is suggested.
Additional results regarding the stability of the laminar backward-facing step flow were reported by Beaudoin et al.[6]. Their experimental study was based on flow visualizations and PIV measurements of the velocity. The geometrical configuration of the experiments was characterized by the relatively low expansion ratio (10/9) and aspect ratio (3/2). The experimental results revealed the presence of longitudinal structures located at the bottom wall, for Reynolds numbers in the range Re=20.. 200. The structures are periodically distributed in the span-wise direction, with a wavelength λ=3 (normalized with the step height) independent of the Reynolds number and the step height (expansion ratio). It was suggested that the presence of these longitudinal vortices are related with a centrifugal instability of the flow. In order to determine the location of the instability, two-dimensional computations were conducted. An inviscid analysis of the centrifugal stability based on the calculation of the Rayleigh number was performed in order to determine the potentially unstable zone. Then, following the examination of the viscosity influence, it is concluded that the centrifugal instability is located close to the reattachment line, downstream of the shear layer.

2. Numerical formulation

The mathematical model used in the present study is represented by the Navier-Stokes equations, for the case of Newtonian fluid with constant density and viscosity. The equations are numerically solved using a finite volume scheme, of second order accuracy in time and space. Details on the numerical procedure can be found in Karimian and Straatman [7].
The computational domain and the Cartesian system of coordinates considered in

the present study are presented in Figure 1. The dimensions of the domain are intended to simulate the geometrical set-up in the experimental study of Beaudoin et al.[6]. The expansion ratio is 10/9 and the aspect ratio of the outlet section is 3/5. The outflow distance was chosen after testing its influence on the reattachment length, at the highest Reynolds number considered in the present study, Re = 565.

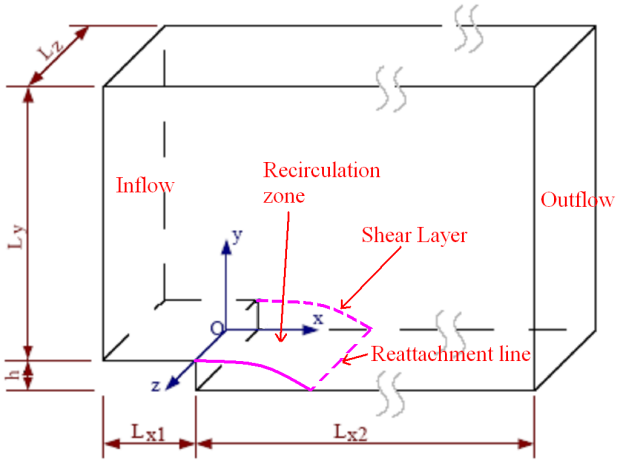

Figure 1. Sketch of the computational domain and of the main elements of a backward-facing step flow

The height of the inlet channel is $L_y = 9h$, where h is the step height. Thus the expansion ratio is $\alpha = (L_y + h)/L_y = 10/9$. The width of the domain is $L_z = 15h$, resulting in an aspect ratio of 3/5. The inlet and outlet surfaces must be far enough from the step in order to avoid the influence of their position on the numerical results. The inlet distance is $L_{x1} = 3h$ and, according to [4], is large enough for the Reynolds numbers considered. The outflow distance is $L_{x2} = 30h$ and it was chosen after testing its influence on the reattachment length, at the highest Reynolds number considered in the present study (Re=565).
The set of boundary conditions imposed to the Navier-Stokes equations is as follows. The upper and lower surfaces were treated as solid walls and the no-slip boundary conditions were used: $u = v = w = 0$. At the outflow boundary the following condition was imposed: $\frac{\partial u}{\partial x} = \frac{\partial v}{\partial x} = \frac{\partial w}{\partial x} = 0; p = 0$. For the lateral boundaries two situations are considered: first the case of solid boundaries when the no-slip conditions are used, and then the case when symmetry boundaries conditions are applied, simulating the case of a flow domain infinite in span-wise direction: $\frac{\partial u}{\partial z} = \frac{\partial v}{\partial z} = 0; w = 0$. At the inlet surface two types of velocity profiles are imposed: *i*) experimental, from the results of Beaudoin et al.[6]; *ii*) Poiseuille profile. The parabolic profile was used only in combination with the symmetry lateral conditions. The computational domain presented in Figure 1 is discretized into hexahedral, orthogonal finite volumes. The grid is refined in the vertical direction close to the horizontal walls and in the longitudinal direction in the recirculation zone. The grid distribution was chosen after conducting grid convergence tests at Re = 565, considering solid lateral boundaries. The total number of the finite volumes is around 3.3 million.
The numerical procedure is validated by comparisons of the reattachment length and velocity profiles with the experimental and numerical results of Beaudoin et al.[6]

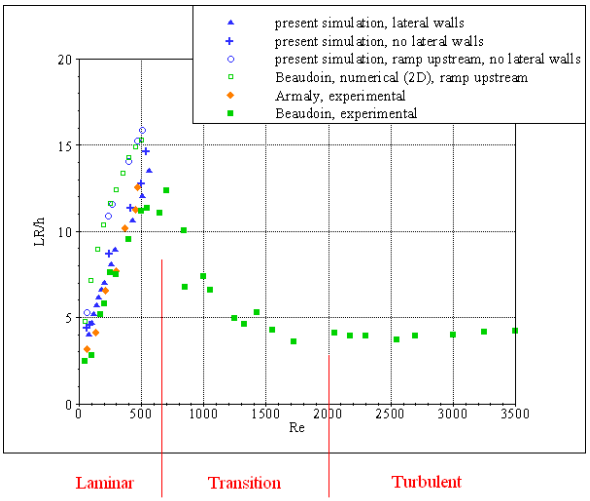

Figure 2. The reattachment length in the symmetry plane vs. the Reynolds number; comparison with other experimental and numerical results

and Armaly et al.[1]. Both cases of no slip and symmetry lateral conditions are considered. The Reynolds number is based on the step height h and the maximum velocity at the step edge, U_0. Figure 2 shows the dependency of the reattachment length L_R in the symmetry plane ($z = 0$) with the Reynolds number. The three flow regimes, laminar, transition and turbulent are identified from the experimental data of Beaudoin et al.[6] The results obtained in the present computational study are in good agreement with the experimental and numerical results reported in [6]. Velocity profiles in the symmetry plane are presented in [8]. They show a good resemblance with the experimental results of Beaudoin et al. [6].

3. Stability considerations

In the present study the problem of centrifugal instability at low Reynolds numbers is investigated, using the same approach as Beaudoin et al.[6], but for the three-dimensional computational domain, considering the case of no-slip and symmetric conditions at the lateral boundaries. Also the influence of the inflow profile on the flow stability is examined.
A sufficient condition for the centrifugal instability of a two-dimensional rotating flow is (Sipp and Jacquin [9]):

$$\Phi = \frac{2V\omega}{R} < 0 \tag{1}$$

where Φ is a generalized Rayleigh discriminant, V is the velocity in the rotation plane, ω is the vorticity and R is the radius of curvature of the streamlines.
This general criterion was used in the present study to determine the zones of potential centrifugal instability. The generalized Rayleigh discriminant was computed in the symmetry plane, where the transverse velocity w and all the derivatives with respect to the z are zero, and thus the flow can be considered locally two-dimensional. Three zones of potential centrifugal instability are found, for all Reynolds numbers considered. The intensity of the potential instability of each region is given by the

corresponding local minimum value of the Rayleigh discriminant ($\Phi_{\min}$). Figure 3 presents the contours of Φ in the symmetry plane ($z = 0$) for Re=100, showing the three potentially unstable zones, identified as I, II, III.

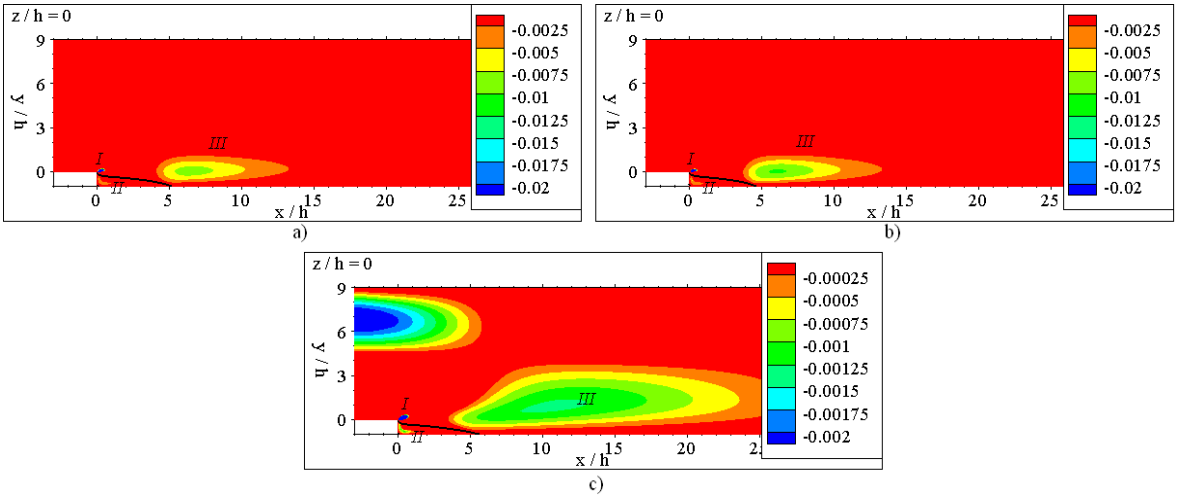

Figure 3. Contours of the Rayleigh discriminant in the symmetry plane (Re=100): a) symmetry lateral conditions; b) no slip conditions; c) Poiseuille inflow profile

The first zone (I) is located near the step edge and it is the least extended. Here the Rayleigh discriminant has a minimum value $\Phi_{\min} \approx -0.15$ which is not affected by Reynolds number or by conditions at lateral boundaries. The second zone (II) is in the recirculation zone, close to the step. Its size and intensity decrease with the Reynolds for Re > 250, ant it disappears at around Re $= 500$. The last region of potential instability (III) is located above and downstream of the reattachment point and it is the most extended. In this case the local minimum value of Φ is strongly influenced by the Reynolds number and also by the conditions at the lateral boundaries.

When a Poiseuille profile is imposed at the inlet, it is found that the absolute value of the Rayleigh discriminant decreases with one order of magnitude. A fourth region where $\Phi < 0$ is present close to the inlet plane. The fact that the Rayleigh discriminant is not zero implies the fact that the flow in the inlet channel is not parallel (the curvature radius R is not infinite). This proves a deviation of the velocity profile from the parabolic shape, caused by the adverse pressure gradient, produced by the expansion of the channel. The non-zero value of the Rayleigh discriminant is enhanced also by the large vertical gradient of the velocity $\partial u/\partial y$, in the central zone of the channel. It is expected that the intensity and the extent of this additional zone is influenced by the position of the inlet plane.

The viscosity on the centrifugal stability is estimated by the Görtler number:

$$G = \frac{V\delta^{3/2}}{\nu R^{1/2}} \tag{2}$$

where V is the magnitude of the velocity velocity, R is the radius of curvature, ν is the kinematic viscosity and δ is the characteristic size of the unstable zone. This size is defined here as the stream-wise width of the contour corresponding to the

half-minimum value of the Rayleigh discriminant ($\Phi_{\min}/2$), similar to Beaudoin et al.[6].
The first two zones of potential instability (I, II) do not increase with the Reynolds number and are not affected by the conditions at the lateral boundaries. Their characteristic sizes (δ) and radii of curvature remain almost the same. Consequently, their corresponding Görtler numbers are also invariant with the Reynolds number and with the lateral boundary conditions, $G_I \approx G_{II} \approx 1$. In the zone III the characteristic size and the radius of curvature are influenced by the Reynolds number and also by the presence of lateral walls. The Görtler number for this zone (G_{III}) monotonically increases with the Reynolds number (Figure 4). It is concluded that the zone III is the most unstable. When a Poiseuille inflow profile is imposed, it was found that the Görtler number is much smaller, showing that a parabolic profile is less favorable to the centrifugal instability.
The centrifugal instability is a three-dimensional mechanism and it is in general responsible for the production and amplification of the stream-wise vorticity. Therefore the vorticity field will be examined in the next section.

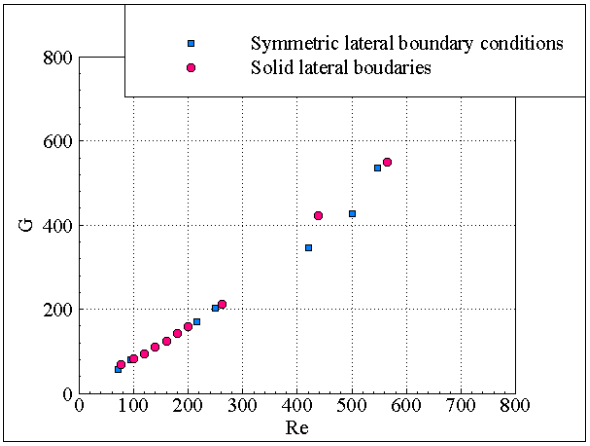

Figure 4. The influence of Re on the Gortler number corresponding to the zone III.

4. Vortex formation

The vorticity field is examined for various boundary conditions imposed at the inlet and lateral frontiers. The goal is to determine the conditions in which longitudinal structures are present in the backward-facing step flow, and what parameters influence their intensity and distribution in the flow domain.
The influence of the sidewalls is first investigated. As a general characteristic of the flows in rectangular channels, pairs of counter-rotating vortices are formed in the vicinity of the walls, upstream of the step. In Figure 5a the contours of the longitudinal vorticity are plotted for Re = 100 in transverse planes, showing the evolution of the longitudinal vortices downstream of the step. Note the formation of two new pairs of stream-wise vortices at the lower corners of the channel: (i) in the immediate vicinity of the step, $x/h = 0.1$; (ii) at $x/h = 6$. As they develop further downstream, these vortices have the tendency to merge with the old vortices of the same sign (i) and to replace the ones of opposite sign, which are pushed towards

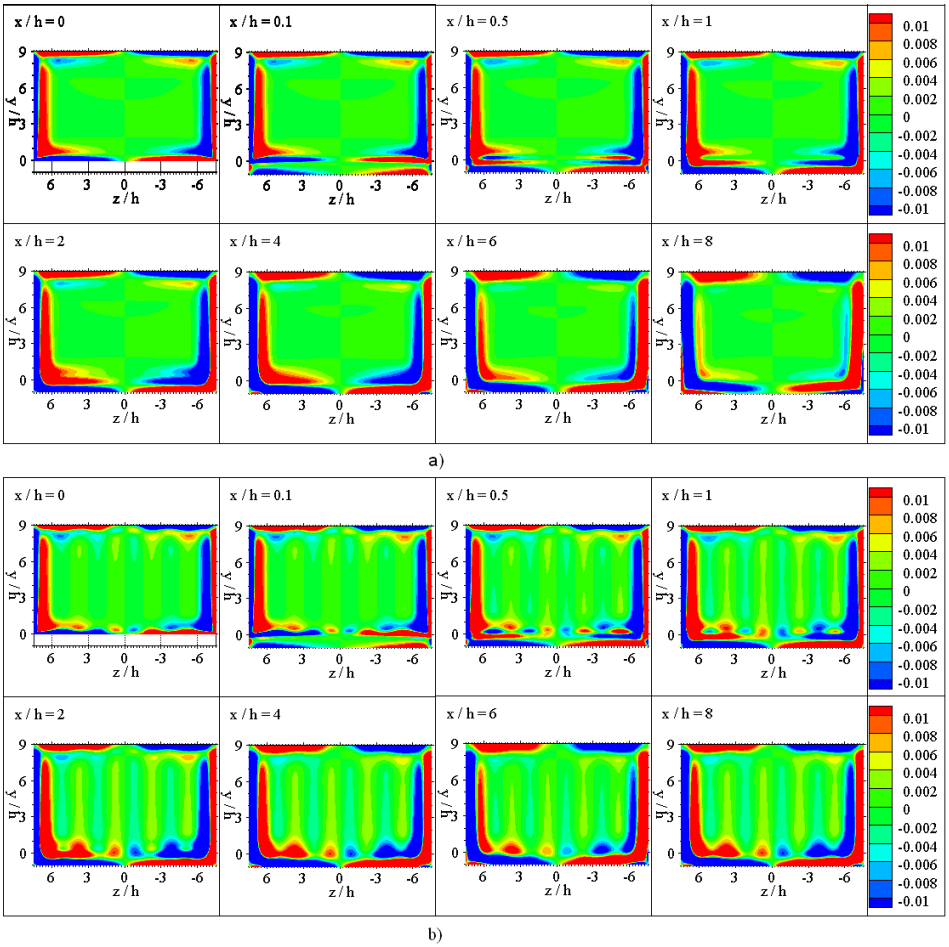

Figure 5. Contours of the stream-wise vorticity at eight stream-wise positions (Re=100): a) produced by sidewalls; b) produced by sidewalls and inflow perturbation ($\lambda/h = 3; \kappa = 0.05$)

the interior of the flow domain (*i* and *ii*). Similar behavior was found for all the Reynolds numbers.

For a quantitative estimation of the vorticity field, transverse profiles were extracted from a horizontal plane below the step level ($y/h = -0.5$), at different stream-wise positions and Reynolds numbers (Figure). The intensity of the vorticity increases with Re in the vicinity of the lateral walls, producing a stronger penetration of the longitudinal structures towards centre of the flow domain. At higher Reynolds numbers the profiles present quasi-periodic oscillations starting from the sidewalls, with the wavelength $\lambda \approx 3h$, independent of Re.

When symmetry boundary conditions are imposed at the lateral planes, no longitudinal vorticity is produced . The influence of perturbations in the inflow velocity is investigated. The experimental and Poiseuille profiles are perturbed withe span-wise periodic disturbances of the form:

$$u'(y,z) = \kappa u_{IF}(y,z)\sin(\frac{2\pi z}{\lambda} + \varphi)$$

where u_{IF} is the inflow velocity in the base and κ is the intensity of the perturbation.

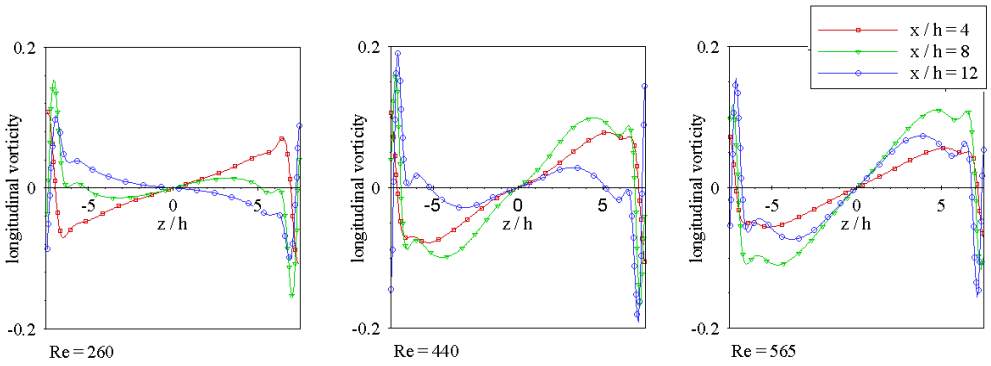

Figure 6. Profiles of the longitudinal vorticity produced by sidewalls in the plane $y/h = -0.5$, at three stream-wise positions (Re= 260; 440; 565).

It is found that the inflow perturbations produce stream-wise vorticity in the boundary layers attached to the top and bottom walls, immediately downstream of the inlet plane. Figure 7 presents the distribution of the stream-wise vorticity produced by a perturbation with the wavelength $\lambda/h = 3$, and the intensity $\kappa = 0.05$ imposed on the experimental and Poiseuille profiles (Re = 100). The contours are presented in vertical and horizontal planes corresponding to the maximum vorticity formation. The vortices produced at the inlet plane are first damped by viscous effects. Downstream of the step, the stream-wise vorticity increases again and span-wise periodical longitudinal structures are formed above the shear layer. The intensity of the vorticity field is much smaller in the case of the parabolic inflow profile.

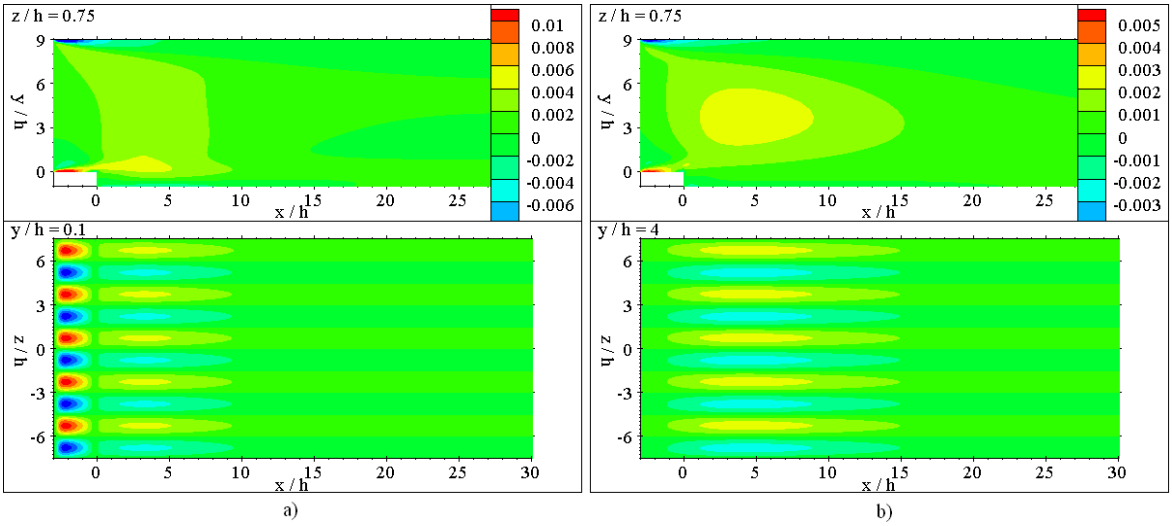

Figure 7. Profiles of the longitudinal vorticity produced by inflow perturabations ($\lambda/h = 3$; $\kappa = 0.05$; Re=100)

The stream-wise variation of the vorticity produced by perturbations of various wavelengths is plotted in Figure 8, for the case of an experimental inflow profile. The profiles are extracted from the horizontal plane $y/h = 0.1$, at span-wise locations where the production of vorticity is maxim. Two tendencies for a local maximum

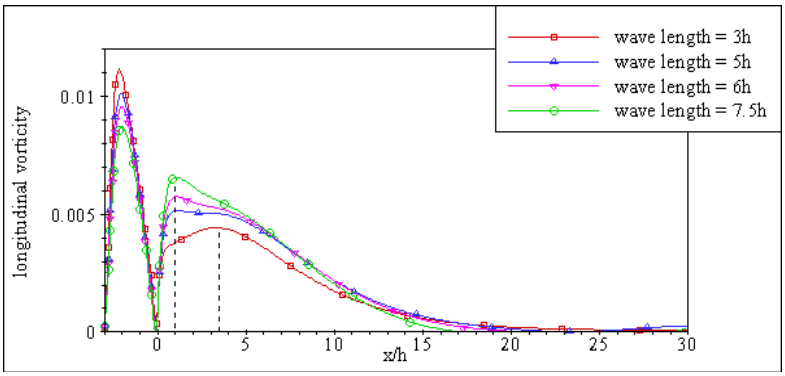

Figure 8. Profiles of the longitudinal vorticity produced by inflow perturbations of various wavelengths ($\kappa = 0.05$; Re=100)

can be noticed downstream of the step. The first is realized only for $\lambda/h = 3$ at the location $x/h \approx 3.5$ and it could be related to the presence of the centrifugal instability in the vicinity of the reattachment. A second local maximum occurs only for the perturbations of higher wavelength ($\lambda/h = 5;\ 6;\ 7.5$) in the vicinity of the step ($x/h \approx 1$). This maximum might be caused by the presence of another instability mechanism in the vicinity of the step, in the shear layer at the separation. Another interesting observation is that the intensity of the original vortices produced in the boundary layer at the inlet is decreasing monotonically with the wavelength of the perturbation, while the amplification of the vorticity downstream of the step increases continuously with λ.
The next step is to find the combined influence of the sidewalls and inflow perturbations. Figure **??** shows how the vortices produced by the lateral walls and by the inflow perturbations interact. It is found that the intensity of the structures is the sum of the intensity produced by the walls when the inflow profile is not perturbed and the vorticity produced by the inflow perturbations in the absence of the sidewalls (Figure 5b).

5. Conclusions

The present study focused on the influence of various conditions imposed at the inflow and lateral boundaries was investigated on the vorticity formation in the back-step flow.
The centrifugal stability in the centre plane was explored, applying inviscid and viscid theory for the stability of rotating fluids. Computing a generalized Rayleigh discriminant, three zones of potential centrifugal instability were found. The influence of the viscosity was estimated by a modified Görtler number, calculated for each of the three zones. It was shown that the most unstable region is situated close to reattachment, downstream of the recirculation zone. The analysis of viscous effects shows that the intensity of the centrifugal instability increases monotonically with the Reynolds number. No significant influence of the sidewalls on the centrifugal stability is found. However, the flow is much more stable when the experimental inflow profile is replaced by a parabolic (Poiseuille) profile.
The conditions in which the stream-wise vorticity is produced and amplified were investigated. It was shown that in the presence of the sidewalls, longitudinal vortices

are present in the vicinity of solid walls, upstream of the step edge. These vortices are convected downstream, and interact with new structures formed at the lower corners of the channel, in the vicinity of the step. If symmetry lateral boundary conditions are applied, longitudinal vorticity is produced only when the profile of the inflow velocity is perturbed. The Poiseuille inflow profile is less favorable to the production of stream-wise vorticity than the experimental profile. An important result is the fact that the longitudinal vortices produced by the sidewalls or by the inflow perturbations are amplified immediately downstream of the step. The influence on the stream-wise vorticity of the centrifugal instability located close to the reattachment is not clear.
Finally, it was found that the presence of the step has an amplifying effect on the stream-wise vorticity. The distribution of the longitudinal vorticity can be manipulated by changing the inflow conditions. Thus, methods for flow control can be sought, aiming for the drag reduction on the step or the enhancement of the mixing in the recirculation zone.

References

[1] Armaly, B.F., Durst, F., Pereira J.C.F. and Schönung, B. 1982 "Experimental and theoretical investigation of backward facing step flow", *Journal of Fluid Mechanics*, Vol. 127, pp. 473-496.

[2] Parviz M. and Kim J 1985 "Application of a fractional-step method to incompressible Navier-Stokes equations", *Journal of Computational Physics.*, Vol. 59, pp .308-323.

[3] Williams, P.T., and Baker, A.J. 1997 "Numerical simulation of laminar flow over a 3D backward-facing step", *International Journal of Numerical Methods in Fluids, Vol. 24, pp. 1159-1183.*

[4] Kaiktsis L., Karniadakis, G.E., and Orszag S. 1991 "Onset of three-dimensionality, equilibria, and early Kim, J. and Moin, P., 1985, "Application of a fractional-step method to incompressible Navier-Stokes equations",.*Journal of Computational Physics*, Vol. 59, pp.308-323.

[5] Barkley, D., Gomes, M.G., and Henderson, R. 2002 "Three-dimensional instability in flow over a backward-facing step",.*Journal of Fluid Mechanics*, Vol. 473, pp.167-190.

[6] Beaudoin, J.-F., Cadot O. and Wesfreid, J.-E. 2004 "Three-dimensional stationary flow over a backward-facing step", *European Journal of Fluid Mechanics B/Fluids*, Vol. 23, pp.147-155.

[7] Karimian, S.A. and Straatman, A.G. 2006 "Discretization and parallel performance of an unstructured finite volume Navier-Stokes solver", *International Journal of Numerical Methods in Fluids,* Vol. 52, pp. 591-615.

[8] Mihaiescu, A. 2007 "Vortex dynamics, stability and control of backward-facing step", Ph.D. thesis in Engineering Science, University of Western Ontario

[9] Sipp, D. and Jacquin, L. 2000 "A criterion of centrifugal instabilities in rotating systems", in Maurel, A. and Petitjeans, P. (Eds.), "Vortex structure and dynamics", Springer, pp. 229-308